Photoproduction of ρ^0 and ρ^- mesons at 3 GeV

P. Bapu, R. Endorf, B. Meadows, and M. M. Nussbaum
Department of Physics, University of Cincinnati, Cincinnati, Ohio 45221*

H. O. Cohn
Oak Ridge National Laboratory,† Oak Ridge, Tennessee 37830

W. M. Bugg, G. T. Condo, and E. L. Hart
Department of Physics, University of Tennessee,† Knoxville, Tennessee 37916

(Received 26 July 1976)

The photoproduction of ρ^0 and ρ^- mesons has been studied at 3 GeV in the reactions $\gamma d \to d\pi^+\pi^-$, $\gamma d \to p_s n\pi^+\pi^-$, and $\gamma d \to p_s p\pi^-\pi^0$. For ρ^0 and ρ^- production in these reactions we present the total and differential cross sections, the decay angular distributions, and the spin density matrix elements. The photoproduction of the ρ^0 is found to be consistent with s-channel helicity conservation and is dominated by natural-parity exchange. The ρ^- meson production has approximately equal natural- and unnatural-parity-exchange contributions. The unnatural-parity-exchange contribution is consistent with one-pion exchange and is used to estimate the value of $\Gamma_{\rho\pi\gamma}$.

I. INTRODUCTION

This paper presents the results of a study of ρ^0 and ρ^- photoproduction in γd interactions at 3 GeV using a linearly polarized photon beam. Our primary interest is the photoproduction of ρ^- mesons on neutrons, since this reaction has not previously been studied in detail with a linearly polarized photon beam. We have also studied ρ^0 photoproduction on deuterons and neutrons for the purpose of comparison.

The photoproduction of ρ mesons using a linearly polarized photon beam allows one to study the production mechanism in much greater detail than with an unpolarized beam. It is possible to measure nine independent density matrix elements of the ρ meson and separate the contributions due to natural-parity $[P=(-1)^J]$ and unnatural-parity $[P=-(-1)^J]$ exchanges in the t channel.[1] The photoproduction of ρ^0 mesons on protons, neutrons, and deuterons has been previously studied using linearly polarized photon beams.[2-5] All of these studies have shown that ρ^0 photoproduction is strongly diffractive. The production mechanism conserves s-channel helicity at small momentum transfer and the t-channel amplitude is dominated by natural-parity exchange.

The reaction $\gamma n \to \rho^- p$ is difficult to study because of its low cross section, the uncertainty of the γ-beam momentum, and the presence of a π^0 in the final state. The ρ^- photoproduction mechanism on neutrons has previously been investigated by the ABHHM collaboration with a bremsstrahlung beam at energies between 1 and 5 GeV.[6,7] Our experiment is the initial investigation of the ρ^- photoproduction mechanism using a linearly polarized photon beam. The SLAC laser beam used in this experiment was advantageous because it is more nearly monoenergetic than other types of photon beams. We have measured the nine independent ρ^- density matrix elements, enabling us to separate the natural- and unnatural-parity-exchange contributions, and thus measure the $\rho\pi\gamma$ width from the unnatural-parity-exchange contribution where one expects pion exchange to dominate.

In Sec. II the experimental procedures employed in this experiment are discussed and the topological and channel cross sections are given. The photoproduction of ρ^0 mesons on deuterons and neutrons is reported and compared to previous experiments in Sec. III. In Sec. IV the results of our study of ρ^- photoproduction are presented. Our conclusions are summarized in Sec. V.

II. EXPERIMENTAL PROCEDURE AND CROSS SECTION

This experiment is based on 150 000 pictures taken in the SLAC 82-in. deuterium bubble chamber exposed to a nearly monoenergetic linearly polarized photon beam of 3 GeV. The beam was produced by Compton backscattering a linearly polarized ruby-laser beam on a 12.5-GeV electron beam. A detailed description of the beam is given in Ref. 8. The energy distribution of the beam determined from the measurement of ~26 000 electron pairs peaked at 3.05 GeV and had a full width at half maximum of 0.5 GeV. The average linear polarization at 3 GeV was calculated to be $(95\pm2)\%$.[9]

The film was double-scanned for all hadronic events with two or more prongs, and electron pairs were counted every 50th frame. The events were classified on the basis of the number of

prongs and the number of identifiable protons. The events were required to be within a corridor of 2 mm width with respect to the photon beam. The scanning efficiencies calculated from the double scan were greater than 99% for all but the two-prong events, which had a scan efficiency of 96%. The lower scan efficiency for the two-prong events is due to the fact that two-prong events with small opening angles were sometimes misidentified as electron pairs.

Hadronic cross sections were determined from the number of hadronic events, n_{events}, the number of electron pairs, n_{pair}, and the known cross section of electron-pair production, σ_{pair}, as given by the relation

$$\sigma(\gamma n \to \text{hadrons}) = (n_{\text{events}}/n_{\text{pair}})\sigma_{\text{pair}}.$$

At 3 GeV, σ_{pair} has been calculated by Knasel[10] to be 19.65 mb within an accuracy of $\pm 0.5\%$. This value has been verified to an accuracy of $\pm 1\%$.[11] The electron pairs were counted every 50th frame within the same fiducial volume as the hadronic events and normalized to the number of frames scanned. The average number of electron pairs per frame was 9.4, which results in microbarn equivalent for this experiment of 72.2 ± 0.6 events/μb.

The number of observed events and the cross sections for each prong topology are listed in Table I. These cross sections have been corrected for scanning losses. The two- and three-prong cross sections were also corrected for events lost due to small projected opening angles causing them to be misclassified as electron pairs. This correction averaged over all two-prong and three-prong events was found to be $(94 \pm 2)\%$ and $(98 \pm 1)\%$, respectively. Corrections due to wide-angle pair production simulating hadron events and events with undetected Dalitz pairs are estimated to be less than 1%.[2] The cross sections for two- and three-prong events decrease with increasing energy from 3 to 7.5 GeV and the cross sections for the higher number of prongs increase.[12,13]

Events were considered candidates for γn or γd interactions if they had an even number of prongs or if they had an odd number of prongs with one of the prongs being identified as a deuteron or a possible spectator proton on the basis of ionization These events were measured on the University of Tennessee spiral reader at Oak Ridge National Laboratory, and on conventional film-plane measuring machines at the Universities of Cincinnati and Tennessee. Geometric reconstruction was done with the program TVGP[14] and kinematic fitting was done with the program SQUAW.[15] The two- and three-prong events were fitted to the following reaction hypothesis:

$$\gamma d \to p_s p \pi^-, \quad (1)$$

$$\gamma d \to p_s p \pi^- \pi^0, \quad (2)$$

$$\gamma d \to p_s n \pi^+ \pi^-, \quad (3)$$

$$\gamma d \to d \pi^+ \pi^-, \quad (4)$$

$$\gamma d \to d \pi^+ \pi^- \pi^0, \quad (5)$$

where p_s represents a spectator proton. Fits to reactions (3)–(5) were not tried for two-prong events with one identified proton or three-prong events with two identified protons. For three-prong events with two protons the slower of the two was considered the spectator. The photon beam was treated as a measured track using the mean values and errors for momentum and angles determined from the measurement of electron pairs. The two-prong events were fitted with the unseen positive track treated as being measured with zero momentum and momentum errors of $\Delta P_x = \Delta P_y = 0.75 \times \Delta P_z = 30$ MeV/c for a proton and $\Delta P_x = \Delta P_y = 0.75 \times \Delta P_z = 40$ MeV/c for a deuteron.

In order to be considered a good fit the χ^2 probability for a hypothesis had to be greater than 0.1%. In addition, the track ionizations from the fit had to agree with the observed track ionizations. It was usually possible by visual inspection of ionization to distinguish between a proton and a π^+ up to a momentum of about 1.4 GeV/c. If an event had both a good 4C and a good 1C fit, the 4C fit was chosen. For those reactions having a spectator proton, its momentum was required to be ≤ 300 MeV/c.

All events having a good fit to reaction (4) were so classified, unless they also had a fit to reaction (1) (the other 4C reaction) with a higher χ^2 probability. However, the number of events ambiguous between reactions (1) and (4) was extremely small. We also included in reaction (4) events which did not have a 4C fit but fitted reaction (3) with an invariant mass $M(pn)$ less than 1884 MeV/c^2 and in the case of the three-prong events, a cos $\theta(p,n)$ greater than 0.95. These events were considered genuine $d\pi^+\pi^-$ events which failed the 4C fit but still had an acceptable 1C fit to $pn\pi^+\pi^-$ with an ef-

TABLE I. Number of observed events and cross sections for two-prong through seven-prong topologies.

Topology	Observed events	Cross section (μb)
2	3550	54.4 ± 2.8
3	8377	119.4 ± 4.1
4	1160	16.1 ± 1.3
5	1415	19.6 ± 1.4
6	58	0.8 ± 0.3
7	56	0.8 ± 0.3

fective pn mass consistent with a deuteron, and a nearly collinear proton and neutron. Such events accounted for 10% of the $d\pi^+\pi^-$ sample and 3% of the $n\pi^+\pi^-$ events.

Events fitting reaction (2) were found to exhibit a narrow peak in the $\cos(\gamma, \pi^0)$ distribution above 0.98. Events in this peak were interpreted as genuine candidates for the reaction $\gamma d \to p_s p\pi^-$ which failed the 4C fit because of beam-momentum uncertainty and instead fitted $p\pi^-\pi^0$ with a spurious π^0 along the beam direction. Therefore for reaction (2) a cut requiring $\cos(\gamma, \pi^0) < 0.98$ was imposed. The correction for the loss of genuine $p\pi^-\pi^0$ events due to this cut, obtained by extrapolation of the $\cos(\gamma, \pi^0)$ distribution below 0.98, is estimated to be 9%.

Events classified as reaction (3) were required to have a neutron momentum greater than the spectator-proton momentum in order to purge events due to γp interactions. The fraction of events with good fits ambiguous between reactions (3) and (5) was less than 2%. Events with good fits ambiguous between reactions (2) and (3), where a positive track could not be distinguished on the basis of ionization between a pion and a proton, were classified as reaction (3). This is reasonable since one would not expect many candidates for reaction (2) to have a large momentum transfer from the target neutron to the final-state proton. Furthermore, the distributions of these ambiguous events were in agreement with the unique events of reaction (3) and in disagreement with those of reaction (2). These ambiguous events, when interpreted as reaction (3), had the same fraction of ρ^0 as the unambiguous events of reaction (3). When interpreted as reaction (2), they had high $M(\pi^-\pi^0)$ masses with large momentum transfers, and, unlike the unambiguous events of reaction (2), no ρ^- signal.

The numbers of observed events, corrected events, and cross sections for the $p_s p\pi^-\pi^0$, $p_s n\pi^+\pi^-$, and $d\pi^+\pi^-$ channels are listed in Table II. The results have been corrected for scanning efficiency and measuring efficiency [(81 ± 2)%]. The correction for kaons incorrectly fitted as pions is less than 1%.[2] The two-prong events and three-prong events with a short positive track were corrected for the loss of events due to small projected opening angles causing them to be misidentified as electron pairs. This correction is sensitive to small values of t and is influenced by the fact that the beam is linearly polarized. The corrections were determined to be (93 ± 3)% and (96 ± 3)% for the two- and three-prong events respectively in the $p_s n\pi^+\pi^-$ channel and (76 ± 7)% and (94 ± 5)% respectively in the $d\pi^+\pi^-$ channel. This correction was unnecessary for the $p_s p\pi^-\pi^0$ channel because of the presence of an identified proton as one of the two prongs, precluding its misidentification as a positron.

Our cross sections for ρ^0 photoproduction in both the coherent and deuteron breakup channels are consistent with prior γd experiments[7,12,13,16] and charge-symmetric γp reactions.[17] As has been noted in γd experiments at 4.3 GeV (see Ref. 12) and 7.5 GeV,[13] this implies that the interference between isoscalar and isovector exchange in these reactions is minimal. The $\gamma d \to p_s p\pi^-\pi^0$ cross section determined in this experiment agrees well with the value reported by the ABHHM collaboration at energies between 2.5 and 3.5 GeV.[17]

III. ρ^0 PRODUCTION

The invariant-mass distributions of $M(d\pi^+)$, $M(d\pi^-)$, and $M(\pi^+\pi^-)$ for reaction (4) are shown in Fig. 1. The dominant feature is the production of ρ^0 seen in the $M(\pi^+\pi^-)$ spectra. In Fig. 2 the invariant-mass plots of $M(n\pi^+)$, $M(n\pi^-)$, and $M(\pi^+\pi^-)$ are shown for the reaction (3). One again observes a large ρ^0 signal in $M(\pi^+\pi^-)$ spectra. The only other possible significant enhancement in the mass plots are in the $M(n\pi^-)$ distribution.

The Dalitz plots for the $d\pi^+\pi^-$ and $n\pi^+\pi^-$ final states were fitted using a maximum-likelihood procedure in which resonances were incoherently added to a phase-space background. The ρ^0 was treated in the fits as a relativistic Breit-Wigner distribution with an energy-dependent width multiplied by a Ross-Stodolsky mass-skewing factor of $(M_\rho/M_{\pi\pi})^n$. It was necessary to incorporate this factor in the fit to account for the obvious low-

TABLE II. Number of observed events, number of corrected events, and cross sections for $d\pi^+\pi^-$, $p_s n\pi^+\pi^-$, and $p_s p\pi^-\pi^0$ channels.

Channel	Observed events	Corrected events	Cross section (μb)
$\gamma d \to d\pi^+\pi^-$	497	711 ± 49	9.8 ± 0.7
$\gamma d \to p_s n\pi^+\pi^-$	1530	2070 ± 100	28.7 ± 1.4
$\gamma d \to p_s p\pi^-\pi^0$	291	408 ± 37	5.7 ± 0.5

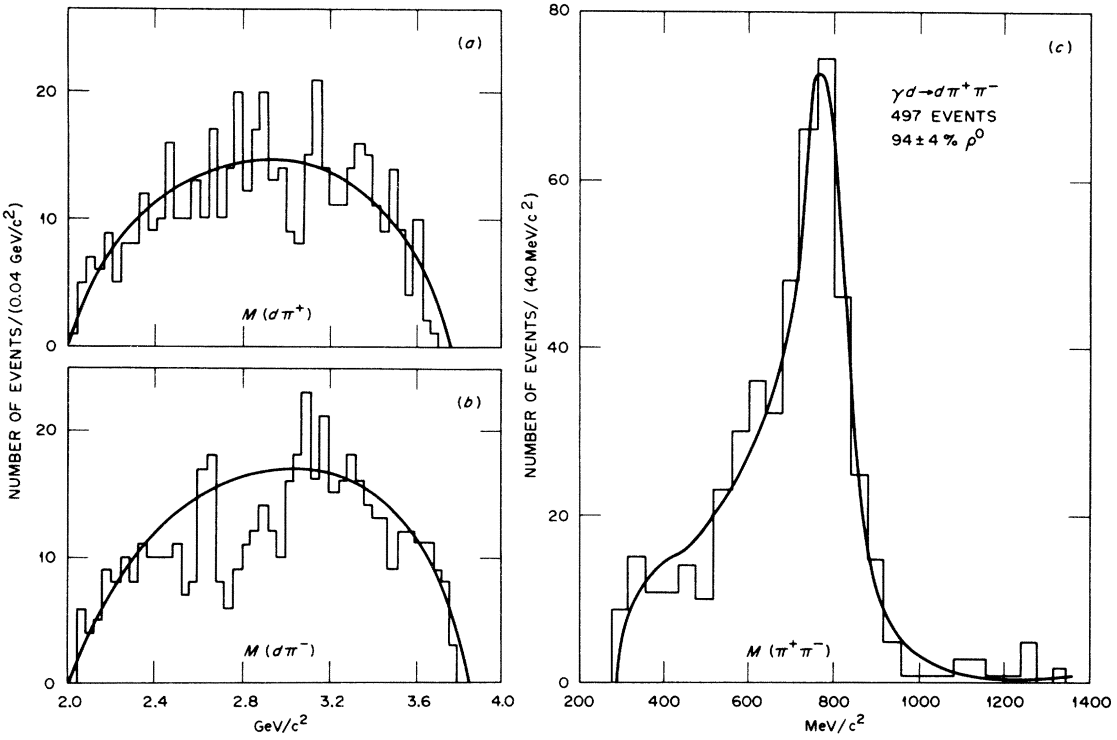

FIG. 1. Invariant-mass distributions for the reaction $\gamma d \to d\pi^+\pi^-$: (a) $M(d\pi^+)$, (b) $M(d\pi^-)$, (c) $M(\pi^+\pi^-)$. The curves are from the maximum-likelihood fit described in the text.

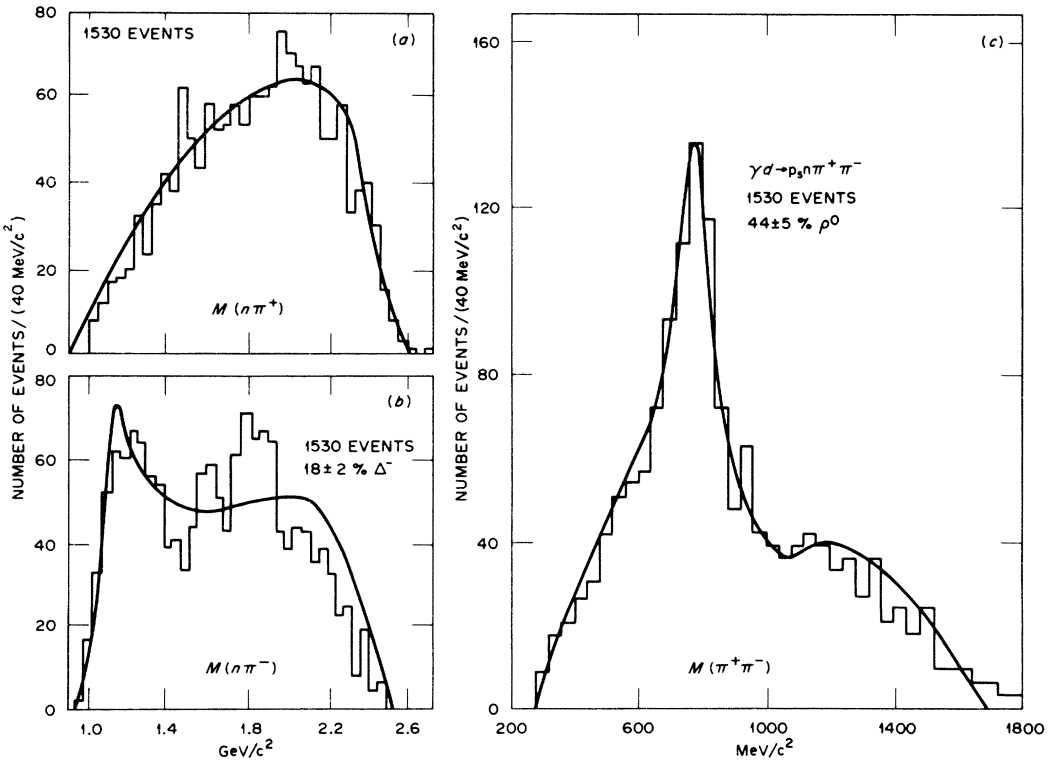

FIG. 2. Invariant-mass distributions for the reaction $\gamma d \to p_s n\pi^+\pi^-$: (a) $M(n\pi^+)$, (b) $M(n\pi^-)$, (c) $M(\pi^+\pi^-)$. The curves are from the maximum-likelihood fit described in the text.

mass skewing of the ρ^0 peak. We do not have sufficient statistics to treat n as a function of momentum transfer as was done in the $\gamma p \to \rho^0 p$ experiments.[2,3] The fits were found to be rather insensitive to variations in n between 3 and 6, but an unacceptable χ^2 was achieved for fits with $n=0$. The ρ^0 mass and width were also fitted. The amount of ρ^0 production determined by the fits was $(94\pm4)\%$ $d\rho^0$ in the $d\pi^+\pi^-$ channel and $(44\pm5)\%$ $n\rho^0$ in the $n\pi^+\pi^-$ channel. The fitted masses and widths for the ρ^0 in these channels are listed in Table III. The curves superimposed on the data in Figs. 1 and 2 are the results of the maximum likelihood fits.

The ρ^0 production cross sections for the channels $\gamma d \to d\pi^+\pi^-$ and $\gamma d \to p_s n\pi^+\pi^-$ were calculated using the percentage of ρ^0 production and the channel cross sections. The correction for events lost owing to small projected opening angles was calculated separately for ρ^0 production in these channels because of its sharp dependence on small momentum transfer. The $\gamma d \to d\rho^0$ and $\gamma d \to p_s n\rho^0$ cross sections were thus determined to be (9.3 ± 0.8) μb and (13.0 ± 1.6) μb, respectively.

Figure 3 shows the momentum-transfer distributions, $d\sigma/dt$, for the reactions $\gamma d \to d\rho^0$ and $\gamma d \to p_s n\rho^0$, where t is the momentum transfer between the incoming γ and the outgoing ρ^0. The $d\sigma/dt$ distributions for $\rho^0 d$ and $\rho^0 pn$ were each fitted to the form $d\sigma/dt = Ae^{-b|t|}$. The values of A and b determined by the fits are given in Table III. Aside from a somewhat smaller slope for coherent ρ^0 photoproduction, there are no substantial differences with previous γd experiments.[4,5,7,16]

To discuss the ρ^0 decay angular distributions, we use the formalism developed to describe vector-meson production by polarized photons.[18,19] The ρ^0 decay angular distribution can be investigated in three reference systems which are distinguished by the choice of the z axis: the helicity system with the z axis along the direction of the

TABLE III. ρ^0 cross section, mass, and width determined from the maximum-likelihood fits for the reactions $\gamma d \to d\rho^0$ and $\gamma d \to p_s n\rho^0$. Also given are A and b from a fit to the ρ^0 differential cross sections of the form $d\sigma/dt = Ae^{-b|t|}$.

	$\gamma d \to d\rho^0$	$\gamma d \to p_s n\rho^0$
σ_{ρ^0} (μb)	9.3 ± 0.8	13.0 ± 1.6
M_{ρ^0} (MeV/c^2)	790 ± 10	800 ± 10
Γ_{ρ^0} (MeV/c^2)	140 ± 10	160 ± 15
A (μb/GeV)	156 ± 30	50 ± 15
b (GeV^{-2})	20.1 ± 2.0	7.4 ± 2.9

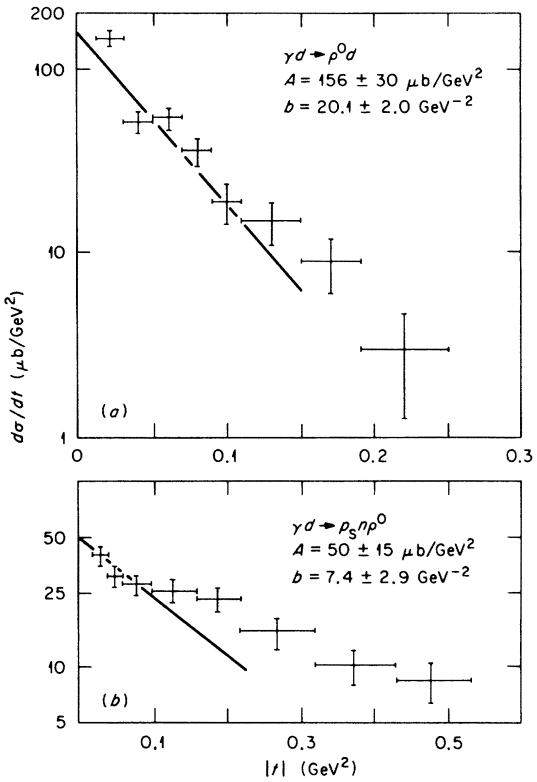

FIG. 3. Momentum-transfer distributions for the reactions (a) $\gamma d \to d\rho^0$. Curve is the best exponential fit in the region 0.01 GeV$^2 < |t| <$ 0.13 GeV^2, (b) $\gamma d \to p_s n\rho^0$. Curve is the best exponential fit in the region 0.02 GeV$^2 < |t| <$ 0.12 GeV^2.

ρ in the total center-of-mass system, the Gottfried-Jackson (GJ) system with the z axis along the direction of the incident γ in the ρ rest frame, and the Adair system with the z axis along the direction of the incident γ in the total center-of-mass system. The preferred system depends on the ρ production mechanism. The helicity system provides the simplest description of s-channel helicity conservation and the GJ system provides the simplest description of t-channel helicity conservation.

The decay angular distribution, $W(\cos\theta, \phi, \Phi)$, of the ρ, produced by linearly polarized photons, is given in all three systems in terms of the nine independent density matrix elements ρ^α_{ij} as

$$W(\cos\theta,\phi,\Phi) = \frac{3}{4\pi}\left(W^{(0)} - P_\gamma \cos 2\phi W^{(1)} - P_\gamma \sin 2\Phi W^{(2)}\right),$$

with

$$W^{(0)} = \tfrac{1}{2}(1-\rho^0_{00}) + \tfrac{1}{2}(3\rho^0_{00}-1)\cos^2\theta - 2\,\mathrm{Re}\rho^0_{10}\sin 2\theta\cos\phi - \rho^0_{1-1}\sin^2\theta\cos 2\phi,$$

$$W^{(1)} = \rho^1_{11}\sin^2\theta + \rho^1_{00}\cos^2\theta - 2\,\mathrm{Re}\rho^1_{10}\sin 2\theta\cos\phi - \rho^1_{11}\sin^2\theta\cos 2\phi\,,$$

$$W^{(2)} = 2\,\mathrm{Im}\rho^2_{10}\sin 2\theta\sin\phi + \mathrm{Im}\rho^2_{1-1}\sin^2\theta\cos 2\phi\,,$$

where P_γ is the degree of linear polarization of the photon, θ and ϕ are the polar and azimuthal angles of the π^+ in the ρ rest frame, and Φ is the angle between the electric vector of the photon and the production plane in the total center-of-mass system.

In Table IV are listed the ρ^0 density matrix elements, ρ^α_{ij}, which are calculated by the method of moments in the helicity system for the $\gamma d \to d\rho^0$ and $\gamma d \to p_s n\rho^0$ reactions. For the $n\rho^0$ reaction a background subtraction was made using the side bands adjacent to the ρ^0 peak. No background subtraction was necessary for the $d\rho^0$ in reaction (4). The ρ^α_{ij} were calculated in the momentum-transfer region $0.02\ \mathrm{GeV}^2 < t < 0.4\ \mathrm{GeV}^2$. For the $d\rho^0$ reaction only the three-prong events were included in the fit because of the loss of two-prong events at low momentum transfer. We do not have sufficient statistics to investigate the behavior of the density matrix elements as a function of momentum transfer. The ρ^0 density matrix elements for both reactions are consistent with the values predicted for s-channel helicity conservation of $\rho^1_{1-1} = -\mathrm{Im}\rho^2_{1-1} = \frac{1}{2}$ and all other $\rho^\alpha_{ij} = 0$.

The parity asymmetry parameter is defined as

$$P_\sigma = \frac{\sigma^n - \sigma^u}{\sigma^n + \sigma^u}\,,$$

where σ^n and σ^u are the cross-section contributions due to natural- and unnatural-parity exchange in the t channel. To leading order in energy, the natural- and unnatural-parity-exchange contributions do not interfere and

$$P_\sigma = 2\rho^1_{-1} - \rho^1_{00}\,.$$

The P_σ values calculated for $d\rho^0$ and $n\rho^0$ are given in Table IV. Both values are nearly equal to unity, implying that natural-parity exchange dominates in these reactions.

For s-channel helicity conservation, the decay angular distribution in the helicity system simplifies. If one defines an angle $\psi = \theta - \Phi$, then the decay angular distribution, $W(\cos\theta, \psi)$, is proportional to $\sin^2\theta\cos^2\psi$ for 100% linear polarization. The $\cos\theta$ and ψ distributions for the $d\rho^0$ and $n\rho^0$ reactions are shown in Fig. 4. The data are consistent with the curves, which are proportional to $\sin^2\theta$ and $1 + P_\gamma\cos 2\psi$, as expected for s-channel helicity conservation and natural-parity exchange.

TABLE IV. ρ^0 spin density matrix elements and parity asymmetry parameter in the helicity system for the reactions $\gamma d \to d\rho^0$ and $\gamma d \to p_s n\rho^0$.

ρ^0_{00}	0.19 ± 0.06	-0.07 ± 0.08
$\mathrm{Re}\,\rho^0_{10}$	0.04 ± 0.06	-0.03 ± 0.07
ρ^0_{1-1}	-0.02 ± 0.06	-0.05 ± 0.07
ρ^1_{11}	0.01 ± 0.06	-0.14 ± 0.09
ρ^1_{00}	-0.01 ± 0.06	0.13 ± 0.07
$\mathrm{Re}\,\rho^1_{10}$	-0.03 ± 0.06	-0.05 ± 0.07
ρ^1_{1-1}	0.34 ± 0.09	0.43 ± 0.10
$\mathrm{Im}\,\rho^2_{10}$	-0.02 ± 0.06	0.01 ± 0.07
$\mathrm{Im}\,\rho^2_{1-1}$	-0.38 ± 0.09	-0.40 ± 0.10
P_σ	0.69 ± 0.19	0.74 ± 0.20

IV. ρ^- PRODUCTION

The invariant-mass distributions for $M(p\pi^-)$, $M(p\pi^0)$, and $M(\pi^-\pi^0)$ are shown in Fig. 5 for reaction (2). A strong ρ^- peak is observed in the $M(\pi^-\pi^0)$ distribution. The only other enhancement is a small $\Delta^0(1236)$ signal in $M(p\pi^-)$.

The $p\pi^-\pi^0$ Dalitz plot was fitted using the same maximum likelihood procedure described in Sec. III, except for the use of a skewing factor which is inappropriate for nondiffractive ρ production. The

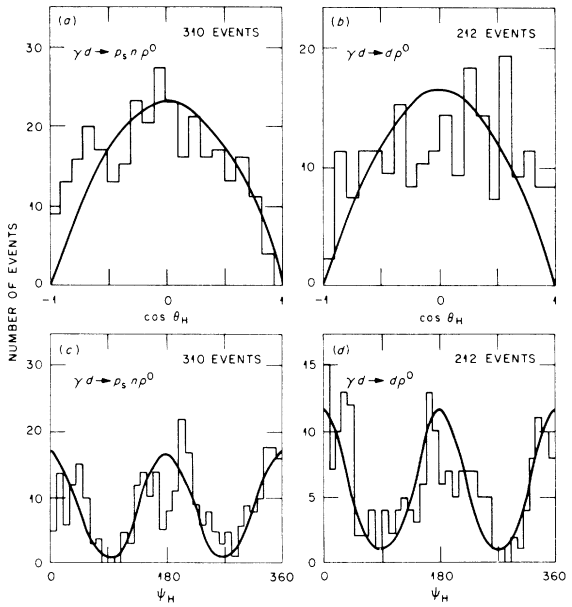

FIG. 4. ρ^0 decay angular distributions of $\cos\theta_H$ in the helicity system for reactions (a) $\gamma d \to p_s n\rho^0$, (b) $\gamma d \to d\rho^0$. Curves are proportional to $\sin^2\theta$. ρ^0 decay angular distribution of ψ_H in the helicity system for reactions (c) $\gamma d \to p_s n\rho^0$, (d) $\gamma d \to d\rho^0$. Curves are proportional to $(1 + P_\gamma\cos 2\psi_H)$.

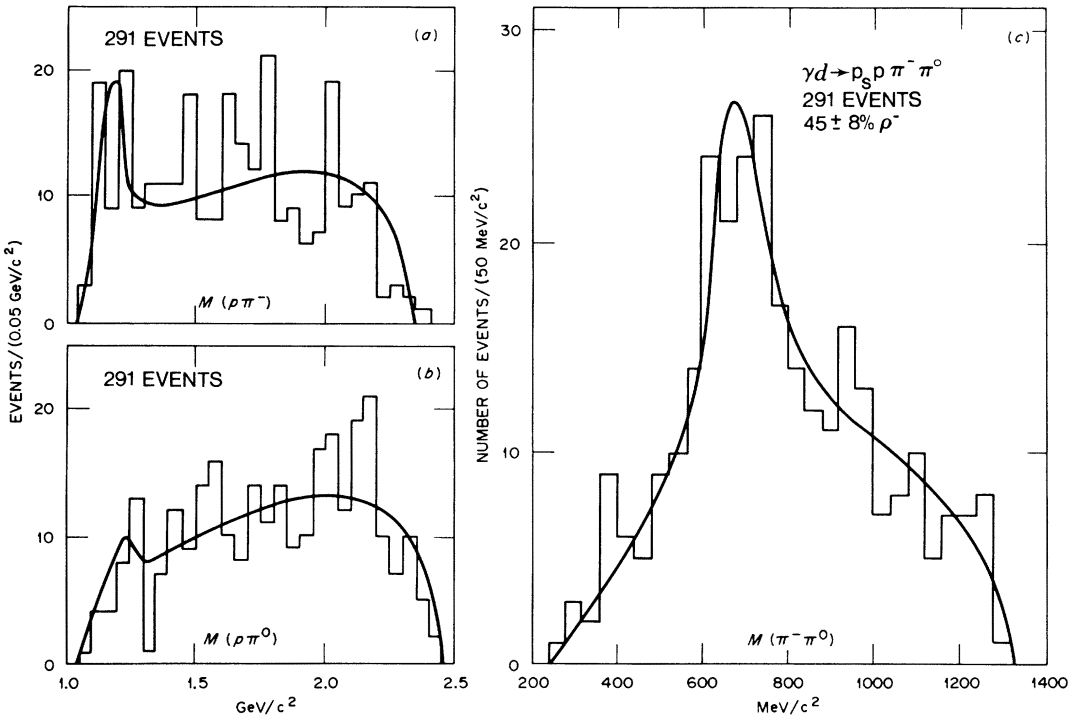

FIG. 5. Invariant-mass distributions for the reaction $\gamma d \to p_s p \pi^- \pi^0$: (a) $M(p\pi^-)$, (b) $M(p\pi^0)$, (c) $M(\pi^-\pi^0)$. The curves are from the maximum-likelihood fit described in the text.

amount of ρ^- production determined by the fit was $(43 \pm 8)\%$, and the fitted ρ^- mass and width are given in Table V. The curves superimposed on the data in Fig. 5 are the result of the maximum-likelihood fit.

The $\gamma d \to p_s p \rho^-$ cross section was determined from the percentage of ρ^- production and the $\gamma d \to p_s p \pi^- \pi^0$ channel cross section to be (2.4 ± 0.5) μb. This value is somewhat higher than that reported by the ABHHM collaboration[7] at energies between 2.5 and 3.5 and considerably larger than the (0.7 ± 0.3) μb reported by Eisenberg *et al.*[16] at 4.3 GeV/c. The principal reason for this distinction is the much greater fraction of ρ^- in the $\pi^-\pi^0$ mass spectrum in our experiment. It should also be noted that our best fit value for the ρ^- width is on the high side of its canonical value, which of course increases our ρ^- cross section.

The momentum-transfer distribution, $d\sigma/dt$, for $\gamma d \to p_s p \rho^-$ is shown in Fig. 6. A fit to the form $d\sigma/dt = Ae^{-b|t|}$ yielded $A = (15 \pm 4)$ μb/GeV^2 and $b = (6.0 \pm 0.7)$ GeV^{-2}. Our slope, b, is significantly larger than the value ($b = 1.9$ GeV^{-2}) found by the ABHHM collaboration[7] at an energy between 1.2 and 2.5 GeV. This may be due to our use of higher-energy photons and/or smaller background in the present experiment. The larger t slope observed in the present experiment more closely follows the expectations of one-pion exchange (OPE) than does the ρ^- photoproduction data at 1.2–2.5 GeV reported by Benz *et al.*[7]

The decay angular distributions for the ρ^- were investigated in both the helicity and GJ systems. In Table VI are listed the ρ^- density matrix elements which were calculated using the method of moments in the helicity and GJ systems for 0.02 GeV$^2 < t < 0.5$ GeV^2. Except for ρ^0_{00}, the matrix elements are all found to be consistent with zero in both systems. The parity asymmetry parameter P_σ was determined to be 0.06 ± 0.10 indicating natural- and unnatural-parity exchanges in the t channel of almost equal amounts. The cross sections for natural- and unnatural-parity exchanges

TABLE V. ρ^- cross section, mass, and width determined from the maximum likelihood fit for the reaction $\gamma d \to p_s p \pi^- \pi^0$. Also given are A and b from a fit to the ρ^- differential cross section of the form $d\sigma/dt = Ae^{-b|t|}$.

σ_{ρ^-} (μb)	2.4 ± 0.5
M_{ρ^-} (MeV/c^2)	805 ± 20
Γ_{ρ^-} (MeV/c^2)	250 ± 70
A (μb/GeV)	15 ± 4
b (GeV^{-2})	6.0 ± 0.7

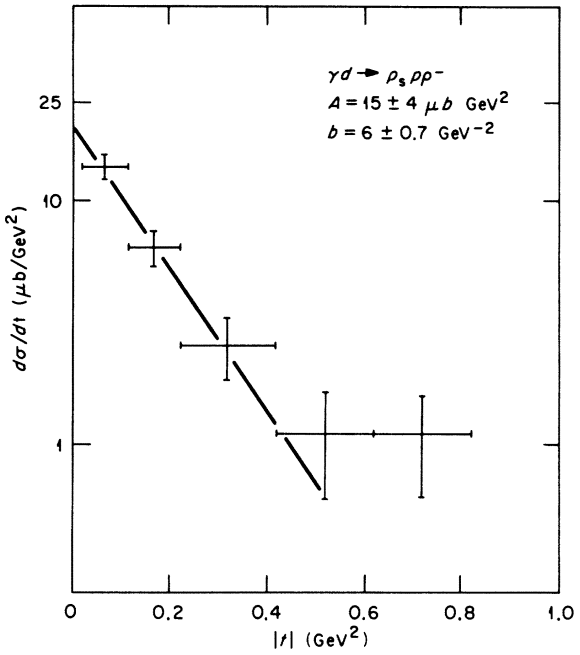

FIG. 6. Momentum-transfer distribution for the reaction $\gamma d \rightarrow p_s p \rho^-$. Curve is the best exponential fit in the region 0.02 GeV^2 < $|t|$ < 0.62 GeV^2.

were determined from the relation $\sigma^{n,u} = \sigma/2(1 \pm P_\sigma)$ to be $\sigma^n = (1.3 \pm 0.3)$ μb and $\sigma^u = (1.1 \pm 0.3)$ μb. This value of σ^u agrees well with the theoretical prediction of the one-pion exchange contribution to the $\gamma n \rightarrow p\rho^-$ cross section at this energy, implying that the unnatural-parity exchange is primarily OPE. The momentum transfer distributions were examined separately for the natural- and unnatural-parity exchanges and were found to be similar. The slope, b, was the same, within errors, for either case.

TABLE VI. ρ^- spin density matrix elements and parity asymmetry parameter for the reaction $\gamma d \rightarrow p_s p \rho^-$.

	Gottfried-Jackson system	Helicity system
ρ^0_{00}	0.36 ± 0.07	0.28 ± 0.07
Re ρ^0_{10}	0.07 ± 0.07	−0.04 ± 0.06
$\rho^0_{1\,-1}$	−0.11 ± 0.06	−0.15 ± 0.06
ρ^1_{11}	−0.05 ± 0.08	0.00 ± 0.08
ρ^1_{00}	−0.12 ± 0.07	−0.22 ± 0.07
Re ρ^1_{10}	0.09 ± 0.07	0.04 ± 0.07
$\rho^1_{1\,-1}$	−0.03 ± 0.09	−0.08 ± 0.09
Im ρ^2_{10}	0.05 ± 0.06	−0.01 ± 0.06
Im $\rho^2_{1\,-1}$	−0.12 ± 0.09	−0.15 ± 0.10
P_σ	0.06 ± 0.11	0.06 ± 0.11

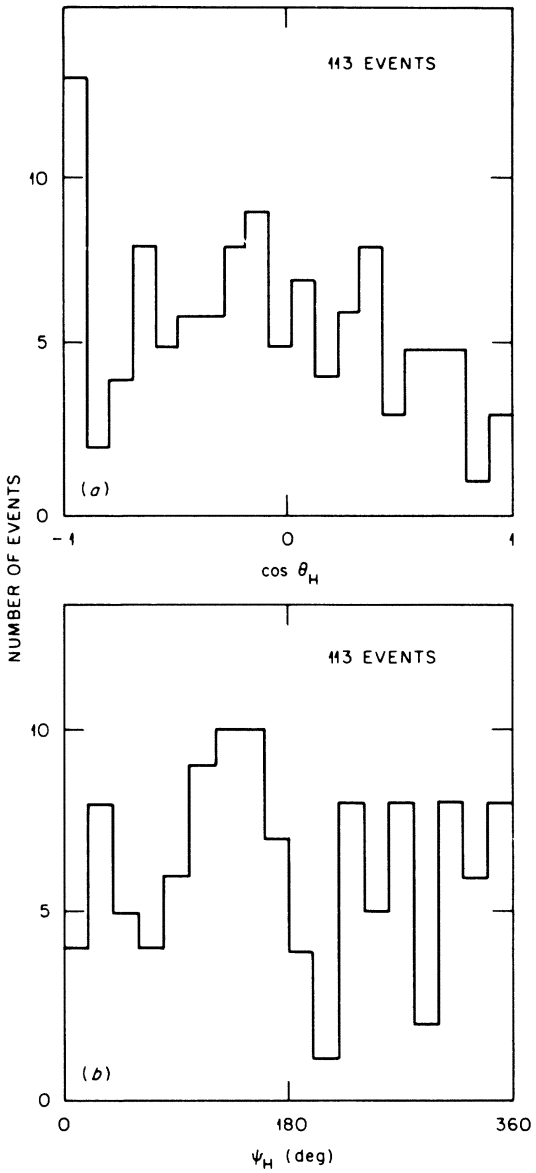

FIG. 7. ρ^- decay angular distribution in the helicity system for the reaction $\gamma d \rightarrow p_s p \rho^-$: (a) cos$\theta_H$, (b) ψ_H.

Figure 7 shows the cos θ and ψ decay angular distributions for the ρ^- in the helicity system. The distributions are all structureless and within the statistics are consistent with being flat. In the helicity system, for 100% linear polarization, $W(\phi)$ is proportional to $\cos^2\phi$ for natural-parity exchange and is proportional to $\sin^2\psi$ for unnatural-parity exchange; therefore a flat $W(\psi)$ distribution indicates equal amounts of natural-and unnatural-parity exchanges, as implied by our value of P_σ.

TABLE VII. Natural- and unnatural-parity exchange ρ^- density matrix elements in the Gottfried-Jackson system for the reaction $\gamma d \to p_s p \rho^-$.

ρ^u_{00}	0.24 ± 0.10
Re ρ^u_{10}	0.16 ± 0.10
ρ^u_{1-1}	0.06 ± 0.10
ρ^u_{11}	0.35 ± 0.10
ρ^n_{00}	0.47 ± 0.10
Re ρ^n_{10}	-0.02 ± 0.10
ρ^n_{1-1}	-0.16 ± 0.10
ρ^n_{11}	0.30 ± 0.10

At high energies the ρ^- density matrix elements can be separated into natural- and unnatural-parity-exchange components using the relation[8]

$$\rho^{n,u}_{\lambda\lambda'} = \tfrac{1}{2}\left[\rho^0_{\lambda\lambda'} \mp (-1)^\lambda \rho^1_{-\lambda\lambda'}\right].$$

The ρ^n_{ij} and ρ^u_{ij} components for the ρ^- are given in Table VII. The GJ system was used since it is the most appropriate system in which to study t-channel particle exchange. The unnatural-parity density matrix components ρ^u_{ij} should be dominated by OPE. The simple OPE model predicts $\rho^u_{00} = \rho^u_{1-1} = \mathrm{Re}\rho^u_{10} = 0$ and $\rho^u_{11} = \frac{1}{2}$. We find that, within rather large errors, ρ^u_{1-1} and $\mathrm{Re}\rho^u_{10}$ are nearly zero and that ρ^u_{11} is close to 0.5. The value for ρ^u_{00} may be nonzero, which could be due to absorption affects or a breakdown, at 3 GeV, of the high-energy approximation used to separate the natural- and unnatural-parity exchanges. It is interesting to note that for the reaction $\gamma p \to \omega p$, where OPE is also considered the main contribution to the unnatural-parity exchange, the spin density matrix element ρ^u_{00} appeared to be significantly nonzero at an energy of 2.8 GeV.[20] For the natural-parity-exchange density matrix elements ρ^n_{ij}, both ρ^n_{00} and ρ^n_{11} seem to be nonzero and ρ^n_{1-1} and $\mathrm{Re}\rho^n_{10}$ are consistent with zero.

An upper limit to the $\rho\pi\gamma$ width, $\Gamma_{\rho\pi\gamma}$, has been estimated by comparing the cross sections for various nondiffractive γN reactions producing a ρ with similar reactions producing an ω and using the known $\omega\pi\gamma$ width, $\Gamma_{\omega\pi\gamma}$.[21] The difficulty is that most of these reactions have significant non-OPE contributions. However, since the unnatural-parity-exchange contributions have been separated for $\gamma p \to p\omega^0$ and $\gamma n \to p\rho^-$ with both reactions appearing to be dominated by OPE, the unnatural-parity-exchange cross sections of $\gamma p \to p\omega^0$ and $\gamma n \to p\rho^-$ can be used to calculate $\Gamma_{\rho\pi\gamma}$. Assuming that the unnatural-parity contributions for these reactions are due entirely to OPE, one finds that

$$\Gamma_{\rho\pi\gamma} = 2\Gamma_{\omega\pi\gamma}\,\frac{\sigma^u(\gamma n \to p\rho^-)}{\sigma^u(\gamma p \to p\omega)}\,.$$

Using our value of $\sigma^u(\gamma p \to p\rho^-)$, the value of $\sigma^u(\gamma p \to p\omega)$ at 3 GeV from Ref. 20, and the latest world average for $\Gamma_{\omega\pi\gamma}$ (see Ref. 22), we obtain $\Gamma_{\rho\pi\gamma} = (190 \pm 60)$ keV. The 60-keV error is statistical and does not reflect systematic errors in this method of calculating $\Gamma_{\rho\pi\gamma}$. Unbroken SU(3) including ω-ϕ mixing predicts a value of $\Gamma_{\rho\pi\gamma} = 160$ keV.[23] A recent model using broken SU(3) prefers a value of $\Gamma_{\rho\pi\gamma} \approx 80$ keV.[24] The latest measurement of $\Gamma_{\rho\pi\gamma}$ using a coherent scattering process reported $\Gamma_{\rho\pi\gamma} = (35 \pm 10)$ keV.[25] Because of the large uncertainty in our value, it is not clear that an inconsistency exists.

V. CONCLUSIONS

We have measured the topological γd cross sections and channel cross sections for the reactions $\gamma d \to d\pi^+\pi^-$, $\gamma d \to p_s n\pi^+\pi^-$, and $\gamma d \to p_s p\pi^-\pi^0$ at 3 GeV. These measurements are consistent with the values determined in previous γd experiments.

The production of ρ^0 mesons has been studied in the reactions $\gamma d \to d\rho^0$ and $\gamma d \to p_s n\rho^0$. The ρ^0 production mechanism in both reactions was found to be dominated by s-channel helicity conservation and natural parity exchange in the t channel.

The cross section for $\gamma d \to p_s p\rho^-$ at 3 GeV has been measured as (2.4 ± 0.5) μb and the slope of the ρ^- differential cross section has been determined to be (6.0 ± 0.7) GeV^{-2}. The contribution of natural- and unnatural-parity exchanges to ρ^- production were found to be approximately equal at 3 GeV. The unnatural-parity-exchange contribution is consistent with one-pion exchange. Comparing our value for the unnatural-parity-exchange contribution of $\gamma n \to p\rho^-$ with that for $\gamma p \to p\omega$ we obtain a $\rho\pi\gamma$ width of (190 ± 60) keV.

ACKNOWLEDGMENTS

We wish to thank the SLAC accelerator operations crew and the 82-in. bubble chamber crew for their assistance in performing this experiment. We also want to acknowledge the valuable help of the scanning and measuring staffs at the University of Cincinnati, Oak Ridge National Laboratory, and the University of Tennessee. Finally, our thanks to Joe Murray and Roger Gearhart of SLAC for making the beam work.

*Work supported by the U. S. National Science Foundation.
†Work supported by the U. S. Energy Research and Development Administration.

[1]K. Schilling *et al.*, Nucl. Phys. B15, 397 (1970).
[2]J. Ballam *et al.*, Phys. Rev. D 5, 545 (1972).
[3]J. Ballam *et al.*, Phys. Rev. D 7, 3150 (1973).
[4]G. Alexander *et al.*, Nucl. Phys. B69, 445 (1974).
[5]Y. Eisenberg *et al.*, Weizman Report No. WIS-75/15 Ph, 1975 (unpublished).
[6]H. G. Hilpert *et al.*, Nucl. Phys. B21, 93 (1970).
[7]P. Benz *et al.*, Nucl. Phys. B79, 10 (1974).
[8]J. J. Murray and P. R. Klein, Report No. SLAC-JN-67-19, 1967 (unpublished).
[9]W. J. Podolsky, Report No. UCRL-20128, 1971 (unpublished).
[10]T. M. Knasel, DESY Report No. 70/3, 1970 (unpublished).
[11]H. Meyer *et al.*, Phys. Lett. 33B, 189 (1970).
[12]Y. Eisenberg *et al.*, Nucl. Phys. B104, 61 (1976).
[13]G. Alexander *et al.*, Nucl. Phys. B68, 1 (1974).
[14]F. T. Solmitz *et al.*, Alverez Group (UCRL) Programming Note No. P-117, 1968 (unpublished).
[15]O. I. Dahl *et al.*, Alverez Group (UCRL) Programming Note No. P-126, 1968 (unpublished).
[16]Y. Eisenberg *et al.*, Nucl. Phys. B42, 349 (1972).
[17]Y. Eisenberg *et al.*, Phys. Rev. D 5, 15 (1972).
[18]K. Schilling *et al.*, Nucl. Phys. B15, 392 (1970); B18, 332 (E) (1970).
[19]R. L. Thews, Phys. Rev. 175, 1749 (1968).
[20]J. Ballam *et al.*, Phys. Rev. D 7, 3150 (1973).
[21]Y. Eisenberg *et al.*, Phys. Rev. Lett. 22, 669 (1969); 23, 1322 (1969).
[22]Particle Data Group, Phys. Lett. 50B, 1 (1974).
[23]N. P. Samios *et al.*, Rev. Mod. Phys. 46, 49 (1974).
[24]B. J. Edwards and A. N. Kamal, Phys. Rev. Lett. 36, 241 (1976).
[25]B. Gobbi *et al.*, Phys. Rev. Lett. 33, 1450 (1974).